Geocenter motion determination and analysis from SLR observations to Lageos1/2

Hongjuan Yu[1] , Krzysztof Sośnica[2], Yunzhong Shen[1]

1. College of Surveying and Geo-informatics, Tongji University, Shanghai 200092, China

2. Institute of Geodesy and Geoinformatics, Wrocław University of Environmental and Life Sciences, Grunwaldzka 53, 50-357, Wrocław, Poland

Introduction

Accurate quantification and analysis of geocenter motion are of great significance to the construction and maintenance of the international terrestrial reference frame and its geodetic and geophysical applications. The origin of the reference frame is determined by using many techniques such as, global positioning system and satellite laser ranging. It should be considered to be determined by a polyhedron composed of stations that constitute the global observation network. These stations are on the crust of the Earth and can only reflected the movement of the crust rather than the instantaneous center of mass (CM) of the Earth. The offset between the origin of the reference frame and the CM is called geocenter motion. Mass transport in the Earth system such as surface water, atmosphere, sea-level changes, Earth tide, mantle convection and liquid core oscillations results in the geocenter motion. Here, the time series of 26-year geocenter motion coordinates (from 1994 to 2020) is determined by using the network shift approach from Satellite Laser Ranging (SLR) observations to Lageos1 / 2. Then, the geocenter motion time series is analyzed by using singular spectrum analysis to investigate the periodic signals and the corresponding physical mechanisms.

Determination Strategy of Geocenter Motion

- The network shift approach is used to determine the Geocenter Coordinates Motion (GCC). The reference frame is realized by imposing minimum constraint conditions(MCs) on the network of stations. The 7-parameter Helmert transformation is used for the transformation of the realized frame and the a priori frame to get the geocenter motion. Because the orbits, station coordinates and EOP are simultaneously estimated, the no-net-rotation (NNR) is mandatory applied to remove singularities and invert the normal equation matrix. Besides, The no-net-translation is typically used for the datum definition of global networks with estimating GCC.
- The processing scheme, models and the estimated parameters are listed in the Table 1 and Table 2.

Table1 Description of the processing scheme and models (Zajdel et al., 2019)

Type of model	Description
Troposphere delay	Mendes-Pavlis delay model (Mendes and Pavlis 2004)
Cut-off angle	3 deg, no elevation-dependent weighting
Satellite center of mass	Station- and satellite-specific (Appleby et al. 2012)
Length of arc	7 days
Data editing	2.5 sigma editing, maximum overall sigma: 25 mm, minimum 10
normal points	per week
Subdaily pole model	IERS Conventions 2010 (Petit and Luzum 2010)
Tidal forces	Solid Earth tide model, Pole tide model, Ocean pole tide model (Petit and Luzum 2010)
Nutation model	IAU 2000
Planetary ephemeris file	JPL DE405
Loading corrections	Ocean tidal loading: FES2004 (Lyard et al. 2006)
Solar radiation pressure	Direct radiation applied with a fixed radiation pressure coefficient CR CR for LAGEOS-1 = 1.13; CR for LAGEOS-2 = 1.11; (Sosnica 2014; Hattori and Otsubo 2018)
Earth orientation parameters	IERS-14-C04 series (a priori), (Bizouard et al. 2018)
Reference frame	SLRF2014 realization of the ITRF2014 (Altamimi et al. 2016)
Earth gravity field	EGM2008 (Pavlis et al. 2012)
Ocean tide model	CSR4.0A (Eanes 2004)

Table 2 Description of the estimated parameters

Estimated parameters	Description
Satellite orbits	One set per 7-day arc 6 Keplerian elements; 5 empirical parameters; A constant along-track acceleration; once-per-revolution parameters in along-track and cross-track
Station coordinates	One set per 7-day arc, X, Y, Z components for every station
Range biases	One set per 7-day arc, only for selected SLR stations according to the ILRS Data Handling File.
Earth rotation parameters	8 parameters per 7-day arc using PWL parameterization; Pole X and Y coordinates and UT1-UTC with one parameter fixed to the a priori IERS-14-C04 series
Geocenter coordinates	One set per 7-day arc

Analysis of Geocenter Motion

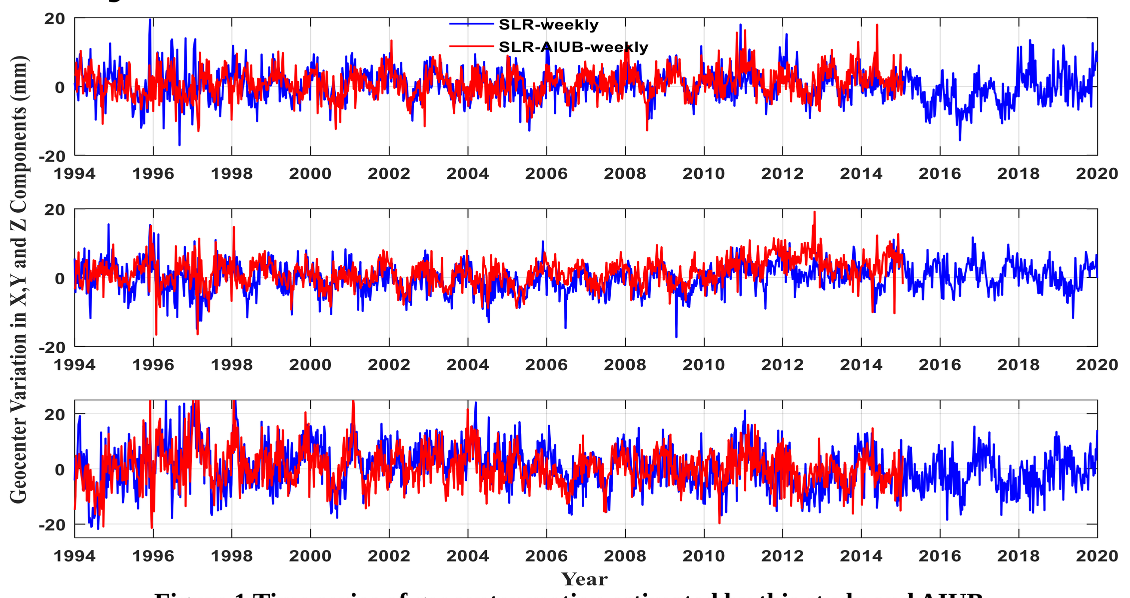

Figure 1 Time series of geocenter motion estimated by this study and AIUB

- In Figure 1-3, “SLR-AIUB-weekly” and “SLR-weekly” denote the Geocenter Motion weekly-solution from Astronomical Institute, University of Bern (AIUB) (http://ftp.aiub.unibe.ch/GRAVITY/GEOCENTER/) and this study. “SLR-AIUB-weekly” is equivalent to internal validation. “SLR-CSR-monthly” denote the Geocenter Motion monthly-solution from Center for Space Research (CSR) (http://download.csr.utexas.edu/pub/slr/geocenter/). “SLR-CSR-monthly” is equivalent to external validation. “smooth” means that 63-day window is used to smooth the GCC series.

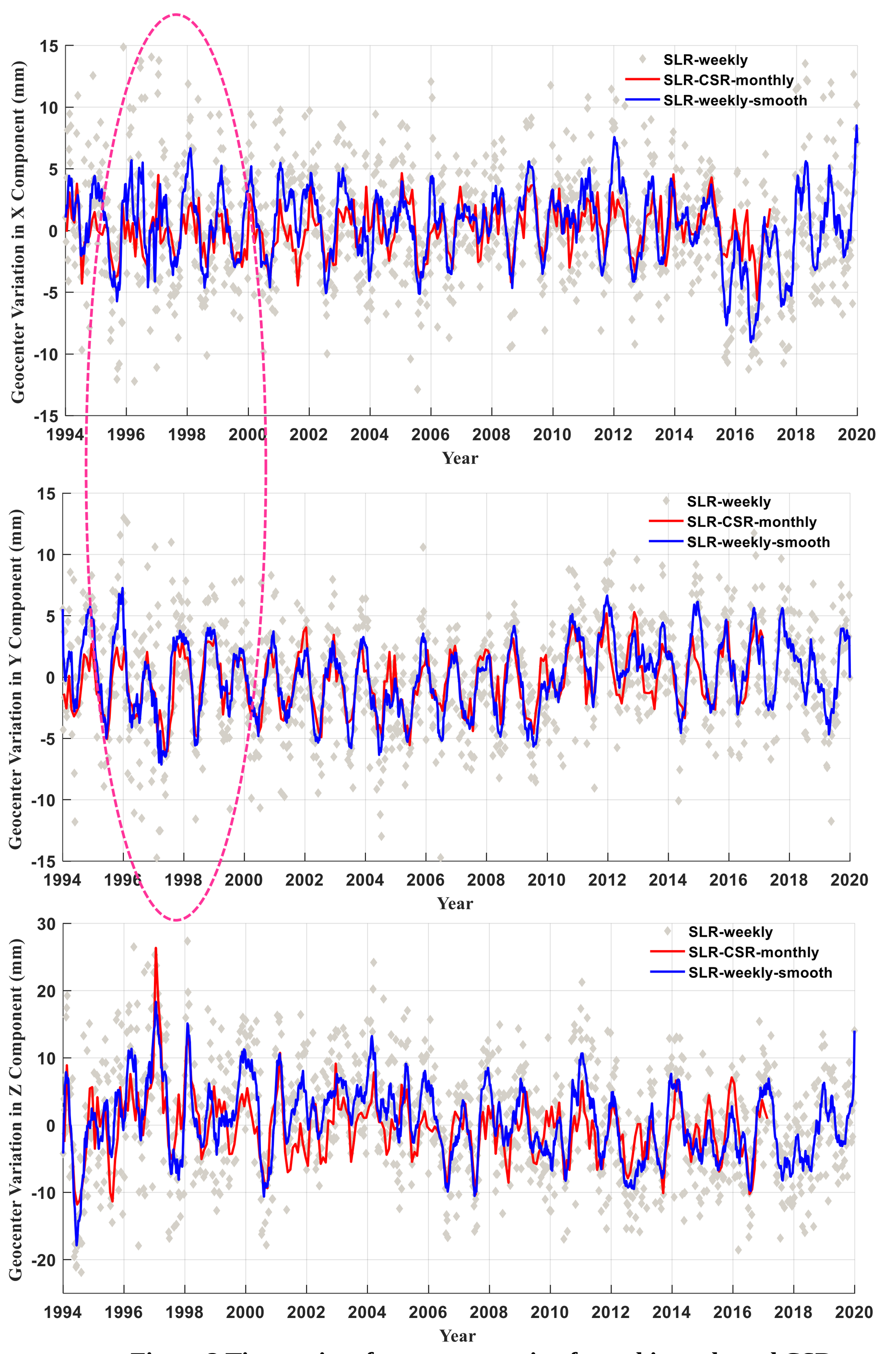

Figure 2 Time series of geocenter motion from this study and CSR

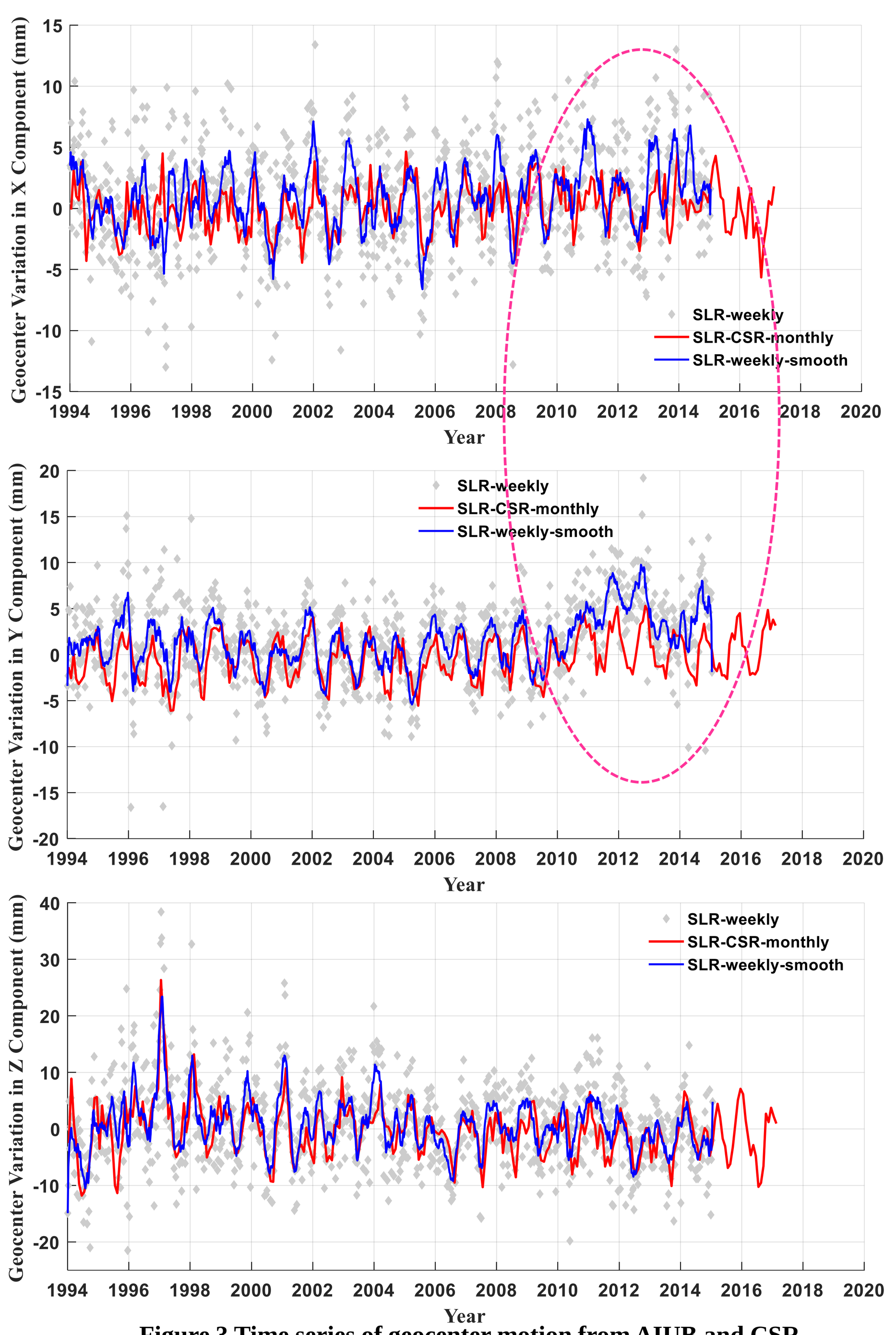

Figure 3 Time series of geocenter motion from AIUB and CSR

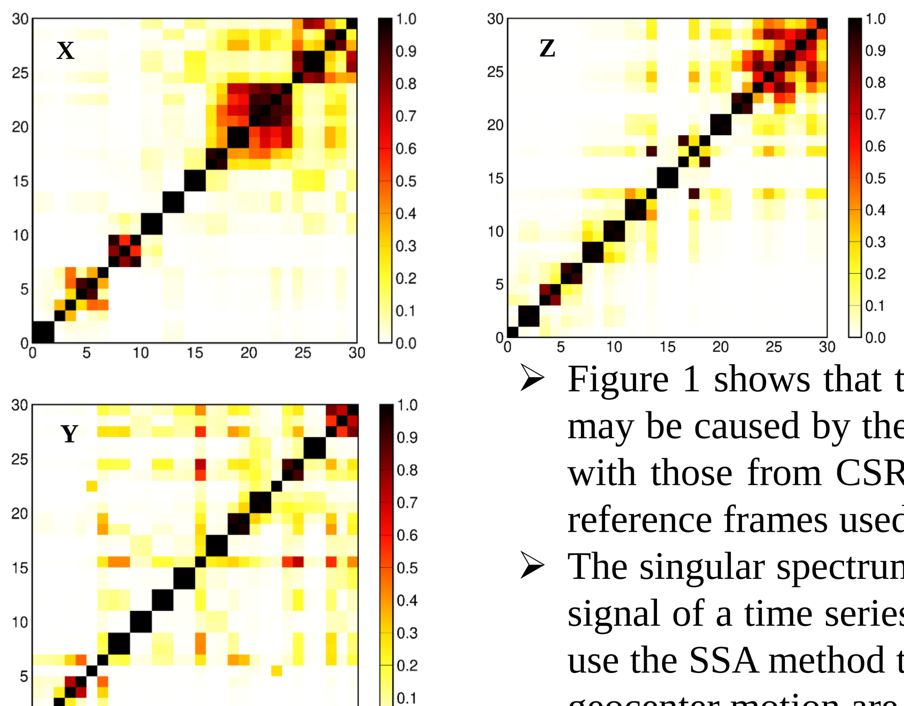

Figure 4 W-correlations for the first 30 orders of the principal components of X, Y and Z component.

- Figure 1 shows that the solution from this study agrees well with that of AIUB. In Figure 2, the solutions in 1997 exist a relatively big deviation, which may be caused by the lack of observations from some core stations. Moreover, the Geocenter Motion series solved by this study have a better consistency with those from CSR. Figure 3 shows an obvious discrepancy between AIUB and CSR in the X and Y components after 2011 due to different a priori reference frames used. However, the Geocenter Motion series from AIUB has a better consistency with those from CSR in the Z component.
- The singular spectrum analysis (SSA) is a powerful and nonparametric spectral estimation method, which can effectively identify and display the periodic signal of a time series, allowing the precise separation and reconstruction of its principal components (w.r.t. the principle, see Wang et al. 2019). Here, we use the SSA method to extract the signals contained in the GCC series to study the physical mechanism that effects the GCC. The principal components of geocenter motion are determined with w-correlation criterion and two principal components with large w-correlation are regarded as the periodic signals as shown in Figure 4. Then the principal periodic components in the X-, Y- and Z- component can be obtained by SSA in Figure 5.

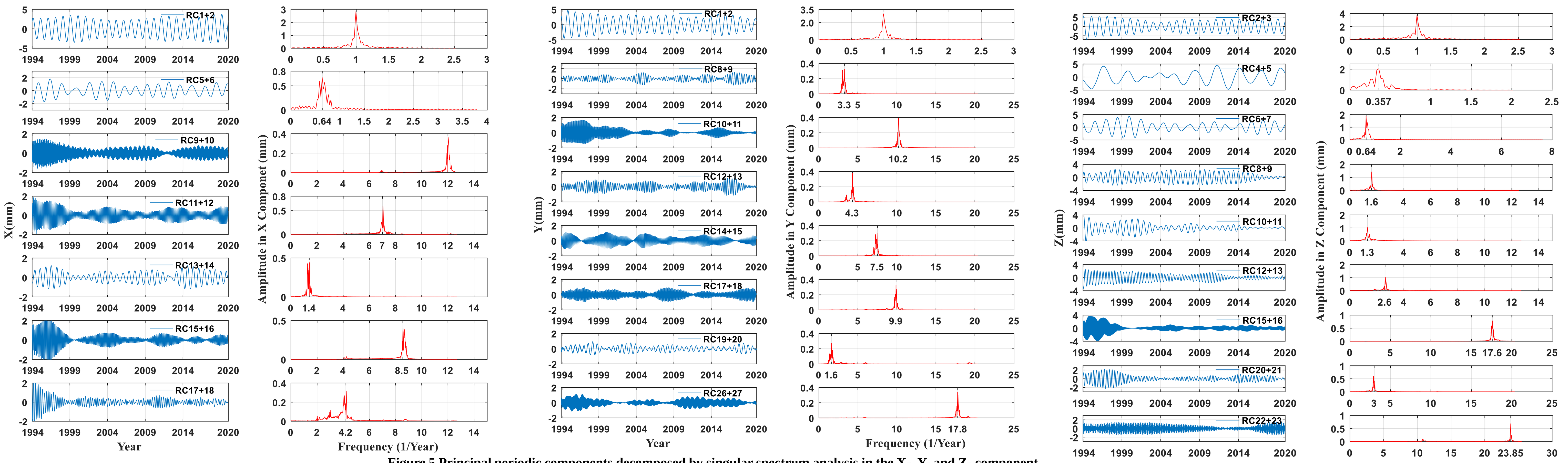

Figure 5 Principal periodic components decomposed by singular spectrum analysis in the X-, Y- and Z- component

Table 3. The periods in the X, Y and Z component detected by SSA.

X		Y		Z	
RC1+2	annual	RC1+2	annual	RC2+3	annual
RC5+6	570 days	RC8+9	3.6 months	RC4+5	1044 days
RC9+10	1 month	RC10+11	1.1 month	RC6+7	570 days
RC11+12	1.7 months	RC12+13	2.8 months	RC8+9	222 days
RC13+14	8.5 months	RC14+15	1.6 months	RC10+11	280 days
RC15+16	1.5 months	RC17+18	1.2 months	RC12+13	140 days
RC17+18	2.8 months	RC19+20	222 days	RC15+16	20 days
		RC26+27	20 days	RC20+21	4 months
				RC22+23	14 days

Table 4 Annual geocenter motion estimates from various approaches (Ries, 2013).

mm	X		Y		Z		
	amp	phase	amp	phase	amp	phase	Reference (comments)
SLR-this study	2.8	31	3.0	292	3.9	52	(7-day estimates, 1994-2020)
SLR-AIUB	2.2	32	2.2	328	3.7	71	Sosnica K. et al., 2014(7-day estimates, 2006-2015)
SLR-CSR	1.7	32	2.8	304	4.3	57	http://download.csr.utexas.edu/pub/slr/geocenter/
SLR (L1/L2)	3.0	35	2.1	319	3.8	65	Drozdzewski M. et al., 2019 (7-day estimates, 2007-2018)
SLR (ILRS)	2.6	40	3.1	315	5.5	22	Altamimi et al., 2011 (ILRS contribution to ITRF2008)
SLR(L1/L2)	2.8	47	2.5	322	5.8	31	Ries, 2016 (60-day estimates; 1993-2016)
SLR(L1/L2)	2.4	55	2.5	321	6.1	31	Ries, 2016 (60-day estimates; 1993-2016) Itrf2014
GPS loading + GRACE +OBP	1.8	46	2.5	329	3.9	28	Wu et al., 2006
GPS loading + GRACE +OBP	2.0	62	3.5	322	3.1	19	Rietbroeck et al., 2011 (updated June 2011)
GPS loading + GRACE +OBP	1.9	25	3.3	330	3.7	21	Wu & Heflin, 2014

- Obvious annual periodic terms and weak periodic oscillations of 1 to 9 months are detectable in all out of three coordinate components. The mass transport of land water is the main factor that causes the seasonal variation of geocenter motion, especially the annual and semi-annual variation.
- A weak sub-millimeter periodic signal of 2.8 months can be detected in both X and Y components, whereas weak periodic oscillations of 222 days and 20 days exist in both Y- and Z components, and the period of 570 days in both X- and Z components. Moreover, a significant periodic signal of about 1044 days, the sub-millimeter periods of 280 days, 140 days and 14 days exist in the Z component.
- The period of 280 days corresponds to the half of draconitic year (560 days) of Lageos-1, to a eclipsing period of Lageos-1, and to the alias period of Lageos-1 with the S2 tide. The period of 14 days and 1044 days equal to the alias period of sub-daily tides (M2) and K1/O1 tide for Lageos-1, respectively. S2 imposes perturbations with a period of 1/2 of the draconitic year of Lageos-1 and M2 with 14 days period and K1/O1 with 1044 days period on the Lageos-1 orbit to effect the GCC. In addition, the period of 222 days just equal to the draconitic year of Lageos-2 and the period of 570 days is the drift of ascending node of Lageos-1.
- Compared to the annual periodic signals of the geocenter motion derived by CSR, both amplitude and phase agree well, except that the amplitude is 1mm larger than that of CSR in the X component.
- The phases of the annual term in the Y and Z components are smaller than those of AIUB, and the amplitudes in all three components are all slightly larger than those of AIUB.

Conclusions and References

- Singular spectrum analysis is effective to detect the periodic signals by decomposing the geocenter motion series.
- Each coordinate component of the 26-year geocenter motion time series contains many seasonal periodic signals. The corresponding physical mechanism of the periodic signals needs further study.
- The estimate of annual geocenter motion in this study is consistent with those from various approaches.

Acknowledgement

The authors gratefully acknowledge the International Satellite Laser Ranging Service for their efforts to collect and provide SLR observations to LAGEOS1/2 satellites, and AIUB and CSR for providing geocenter motion products. This work is mainly supported by National Natural Science Foundation of China (Projects No. 41731069 & 41974002).

- Altamimi Z, Rebischung P, Métivier L, et al. ITRF2014: A new release of the International Terrestrial Reference Frame modeling nonlinear station motions[J]. Journal of Geophysical Research: Solid Earth, 2016, 121(8): 6109-6131.
- Appleby G, Otsubo T, Pavlis E C, et al. Improvements in systematic effects in satellite laser ranging analyses-satellite centre-of-mass corrections[C]//EGU general assembly conference abstracts. 2012, 14: 11566.
- Bizouard C, Lambert S, Gattano C, et al. The IERS EOP 14C04 solution for Earth orientation parameters consistent with ITRF 2014[J]. Journal of Geodesy, 2019, 93(5): 621-633.
- Dro˙zd˙zewski M, So´ snica K, Zus F, Balidakis K (2019) Troposphere delay modeling with horizontal gradients for satellite laser ranging. J Geod. https://doi.org/10.1007/s00190-019-01287-1.
- Eanes RJ. CSR4.0A global ocean tide model. Center for Space Research, University of Texas, Austin,2014.
- Mendes V B, Pavlis E C. High-accuracy zenith delay prediction at optical wavelengths[J]. Geophysical Research Letters, 2004, 31(14).
- Lyard F, Lefevre F, Letellier T, et al. Modelling the global ocean tides: modern insights from FES2004[J]. Ocean dynamics, 2006, 56(5-6): 394-415.
- Pavlis N K, Holmes S A, Kenyon S C, et al. The development and evaluation of the Earth Gravitational Model 2008 (EGM2008)[J]. Journal of geophysical research: solid earth, 2012, 117(B4).
- Petit G, Luzum B. IERS conventions (2010)[R]. BUREAU INTERNATIONAL DES POIDS ET MESURES SEVRES (FRANCE), 2010.
- Sośnica K, Jäggi A, Thaller D, et al. Contribution of Starlette, Stella, and AJISAI to the SLR-derived global reference frame[J]. Journal of geodesy, 2014, 88(8): 789-804.
- Ries, J. C. Reconciling estimates of annual geocenter motion from space geodesy, 20th International Workshop on Laser Ranging, 10-14 October 2016, Potsdam, Germany.
- Ries J C. Annual geocenter motion from space geodesy and models[C]//AGU Fall Meeting Abstracts. 2013.
- Rietbroek R, Fritsche M, Brunnabend S E, et al. Global surface mass from a new combination of GRACE, modelled OBP and reprocessed GPS data[J]. Journal of Geodynamics, 2012, 59: 64-71.
- Wang F, Shen Y, Chen Q, Li W. A heuristic singular spectrum analysis method for suspended sediment concentration time series contaminated with multiplicative noise. Acta Geodaetica et Geophysic, 2019,.
- Wu X, Heflin M B, Ivins E R, et al. Seasonal and interannual global surface mass variations from multisatellite geodetic data[J]. Journal of Geophysical Research: Solid Earth, 2006, 111(B9).
- Wu X, Heflin M B. Global surface mass variations from multiple geodetic techniques – comparison and assessment, Eos Trans. AGU, 88(52), Fall Meet. Suppl., Abstract G31A-01, 2014.
- Zajdel R, Sośnica K, Dach R, et al. Network effects and handling of the geocenter motion in multi-GNSS processing[J]. Journal of Geophysical Research: Solid Earth, 2019, 124(6): 5970-5989.
- Zajdel R, Sośnica K, Drożdżewski M, et al. Impact of network constraining on the terrestrial reference frame realization based on SLR observations to LAGEOS[J]. Journal of Geodesy, 2019, 93(11): 2293-2313.

yuhongjuan123@163.com May 06, 2020